

Symmetric, Optimization-based, Cross-element Compatible Nodal Distributions for High-order Finite Elements

Julian M. Kaufmann^{a,1}, Matthew J. Zahr^{a,2,*}

^a*Department of Aerospace and Mechanical Engineering, University of Notre Dame, Notre Dame, IN 46556, United States*

Abstract

In high-order and high-dimensional finite elements, ill-conditioned nodal distributions are often computationally cost-prohibitive. As a result, uniform distributions quickly fall apart. For tensor-product like elements, Gauss-Legendre-Lobatto (GLL) nodal distributions are often used as a substitute. Besides these, other efficient nodal distributions are difficult to create due to a desired symmetry within elements and conformity with neighboring elements. In this paper, we provide a general framework to construct symmetric, well-conditioned, cross-element compatible nodal distributions which can be used for high-order and high-dimensional finite elements. Starting from the inherent symmetries in any potential element, the framework is used to build up nodal groups in a structured and efficient manner utilizing the natural coordinates of each element, while ensuring nodes stay within the elements. By constructing constrained symmetry groups, the vertices, edges, and faces, of all elements are required to conform to their respective lower-dimensional distributions. Optimizing over these groups yields the desired optimized nodal distributions. We demonstrate the strength of this framework by creating and comparing optimized nodal distributions with GLL distributions (in elements such as the line, quadrilateral, and hexahedron), and its robustness by generating optimized nodal distributions for otherwise difficult elements (such as the triangle, tetrahedron, and triangular prism).

1. Introduction

Finite element methods are ubiquitous in modern numerical analysis. In order to ensure fast and accurate convergence, finite element meshes require well-conditioned mass matrices and other operators. These, in turn, stem from optimal nodal distributions within elements in the mesh.

The most basic nodal distributions are uniform. However, these quickly become ill-conditioned for higher polynomial degree. Another typical nodal distribution is the Gauss-Legendre-Lobatto distribution (GLL). Although highly effective for one-dimensional elements, and thus useful for elements having tensor product structures, it is extremely difficult to adapt these distributions to extruded and simplex-like elements.

Optimal nodal distributions must also have many other properties. Besides resulting in well-conditioned operators, it is also useful for nodal distributions to be symmetrical. This allows elements to be placed in any orientation within the mesh, and does not hinder with computations with boundaries. Finally, it is also helpful for nodal distributions to be somewhat consistent across elements. While creating multi-element meshes, it is incredibly helpful for the vertices, edges, and faces to conform across elements. As a result, well-conditioned, efficient, high-degree, symmetric, and cross-element conforming nodal distributions are highly desired.

In past work, near optimal nodal distributions have been researched extensively for element types such as the line [3], [5], and the triangle [7]. These methods explicitly define potentially non-symmetric nodal distributions for such elements. Further research has been done on the class of all simplices [1], [9], [11]. A special class of points, called Fekete Points [6], have also been studied extensively for the triangle [16] and for the cube [2]. Besides this, spectral methods have also been used for triangles, quadrilaterals, mixed

*Corresponding author

Email addresses: jkaufma2@nd.edu (Julian M. Kaufmann), mzahr@nd.edu (Matthew J. Zahr)

¹Undergraduate, Department of Aerospace and Mechanical Engineering, University of Notre Dame

²Assistant Professor, Department of Aerospace and Mechanical Engineering, University of Notre Dame

triangle-quadrilateral meshes, triangular prisms, and general elements [8], [12], [13], [15], [17]. Although little research has been done on symmetric nodal distributions, symmetric quadrature rules have also been widely studied [4], [14], [18], [19].

Our approach creates a general framework for generating nodal distributions that takes into account inherent symmetries of the elements by constructing the optimized nodes through symmetry groups [19]. Utilizing the generality of the framework, fixed symmetry groups were introduced. These allowed fixing nodes on vertices, edges, and faces of elements, creating compatible nodal structures across different element types. This allows for multi-type meshes. Using the Lebesgue constant as an optimization criterion for well-conditioned operators [10] this framework generated high-order nodal distributions for any generic elements. Nodal distributions for the line (up to polynomial degree 30), the triangle and quadrilateral (up to polynomial degree 16), and the tetrahedron, hexahedron, and triangular prism (up to polynomial degree 7) were generated to show the strength and robustness of this framework. These were compared to existing distributions and plotted for visualization.

2. Symmetry Orbits

2.1. Basic Notions

To construct inherently symmetric distributions, the nodal distributions were organized with respect to symmetry orbits. These symmetry orbits utilize the inherent, or natural, structure of each given element. Because of this, it is useful to define the symmetry orbits in terms of potentially different, natural coordinates, denoted by λ . First, a mapping from these natural coordinates to the physical, or reference (denoted by z) was defined. In general, it takes the form:

$$R : \lambda \rightarrow z \quad (1)$$

$$\lambda \mapsto N\lambda + \nu = z \quad (2)$$

Where λ is a vector of size k , N is a matrix of size $n \times k$ and ν and z are vectors of size n . It should be noted that this map, R , is unique for each element, but applies to all symmetry groups.

To obtain symmetric groups of nodes in natural coordinates from a given parameter, a symmetry orbit is used. Each symmetry orbit maps a set of l parameters, denoted by a vector ξ , to a set of m points. Each of these points is denoted by λ , in natural coordinates. In particular, this is a collection of maps, indexed by $1 \leq i \leq m$:

$$p_i : \xi \rightarrow \lambda \quad (3)$$

$$\xi \mapsto S_i \xi + \sigma_i = \lambda \quad (4)$$

where S_i is a matrix of size $d \times l$ and σ_i and λ are vectors of size d . Since each element has multiple symmetry orbits and symmetry orbits are different across elements, these matrices and vectors also depend on which symmetry orbit is being dealt with. So, to make this explicit, let

$$S_i = S_{k,i} \quad \sigma_i = \sigma_{k,i} \quad (5)$$

denote S_i and σ_i for the i th symmetry orbit, when the element is clear. The dependence on i is dropped when the symmetry orbit is clear. In a large majority of settings, the total point distribution is much more important than any individual map. To account for this, a mapping from ξ to all the resulting points is defined for each symmetry orbit:

$$P : \xi \rightarrow \bar{\lambda} \quad (6)$$

$$\xi \mapsto [p_1(\xi) \mid p_2(\xi) \mid \dots \mid p_m(\xi)] = \bar{\lambda} \quad (7)$$

Where ξ , S_i , and σ_i are as defined above, and $\bar{\lambda}$ is a matrix of size $d \times m$ denoting a collection of m points in natural coordinates. As general notation, a bar on a variable will symbolize a collection of objects, which will be assumed to have been combined in the natural way when no confusion can arise.

In general, this means each symmetry orbit maps a set of parameters to a set of points given in terms of the natural coordinates of the associated element. To make the dependence on the symmetry orbit and element type explicit, let

$$P = P_k^Q(\xi) \quad (8)$$

denote the k^{th} symmetry orbit of element type Q with parameters ξ . Two important parameters are associated with each symmetry orbit, namely the number of points it outputs (which is the same as the maximum for the index i above),

$$\text{Card}(P_k^Q) \quad (9)$$

and the length of the vector ξ it takes in (which is the same as the dimension of the source space of P),

$$\text{Dim}(P_k^Q) \quad (10)$$

Symmetry orbits for many basic elements, along with their cardinality and dimension were computed and written down. Many symmetry orbits for basic elements were taken from [19].

2.2. Constrained Symmetry Orbits

Oftentimes, it is desired to restrict where within the domain of the element the resulting points can lie. This is especially useful when it is desired to have a certain number of points on edges or faces, or when the desired resulting location of a few point is already known (such points will be called fixed points in the future). The simplest way to enforce these restrictions is by restricting the parameters, ξ . Rather than attempting to recalculate what each ξ should be in each symmetry orbit in each element for the desired behaviour, it is more helpful to define another mapping from constrained parameters, α to the original parameters, ξ .

$$\tilde{P}(A, b) : \alpha \rightarrow \xi \quad (11)$$

$$\alpha \mapsto A\alpha + b = \xi \quad (12)$$

as explicitly shown here, each constrained mapping has a dependence on the matrix A and vector b . It should be noted that the size of b , ξ , and the number of rows of A should have the same size, say k , but the number of columns of A and the size of α may be any natural number less than or equal to k . This implies that the number of constrained parameters may indeed be less than the number of parameters. In fact, in the simple example of requiring the resulting nodes to be on the top face of a 2D Quadrilateral, one of the parameters must be 1, but the other can vary. So, there is only one constrained parameter, but two resulting parameters.

In total, for a choice of element, symmetry orbit, and matrix A and vector b we have a string of mappings:

$$\alpha \xrightarrow{\tilde{P}(A, b)} \xi \xrightarrow{P_k^Q} \bar{\lambda} \xrightarrow{R} \bar{z} \quad (13)$$

where the last mapping is assumed to act on each column of the resulting $\bar{\lambda}$ resulting in a matrix of physical coordinates. It is often helpful to talk about the composition of all of these mappings,

$$\tilde{P}_k^Q(A, b) : \alpha \rightarrow \bar{z} \quad (14)$$

$$\alpha \mapsto R \circ P_k^Q \circ \tilde{P}(A, b)(\alpha) \quad (15)$$

By abuse of notation, if $A = Id.$ and $b = \mathbf{0}$, we denote $\tilde{P}_k^Q(A, b)$ by P_k^Q , its unconstrained map. The dimension and cardinality of constrained symmetry orbits may also be easily calculated:

$$\text{Card}(\tilde{P}_k^Q(A, b)) = \text{Card}(P_k^Q) \quad (16)$$

$$\text{Dim}(\tilde{P}_k^Q(A, b)) = \text{col}(A) \quad (17)$$

where $\text{col}(A)$ denotes the number of columns of A . It should be noted that this definition does agree with the previous definition of dimension when A is the zero matrix of correct size.

2.3. Symmetry Orbit Collection

In order to optimize over large sets of nodes, it is helpful to define the notion of a Symmetry Orbit Collection. In general, this is a collection of both unconstrained and constrained symmetry orbits:

$$\mathbb{P} = (\tilde{P}_{k_1}^Q(A_1, b_1), \tilde{P}_{k_2}^Q(A_2, b_2), \dots, \tilde{P}_{k_n}^Q(A_n, b_n)) \quad (18)$$

and define the union of two such sets, $\mathbb{P} \cup \mathbb{P}'$ as simply the concatenation of all $\tilde{P}_{k_i}^Q(A_i, b_i)$ in both sets. These types of collections naturally induce maps from a vector of parameters of size $\sum_{i=1}^n \text{Dim}(\tilde{P}_{k_i}^Q(A_i, b_i))$ to a collection of points in the physical domain. The parameter vector, $\bar{\alpha}$ is simply a stacking of all the α vectors needed for each symmetry orbit. Namely,

$$\bar{\alpha} = \begin{bmatrix} \alpha_1 \\ \alpha_2 \\ \vdots \\ \alpha_n \end{bmatrix} \quad (19)$$

where each α_i is a vector of size $\text{Dim}(\tilde{P}_{k_i}^Q(A_i, b_i))$. So, the induced mapping is defined as:

$$\mathbb{P}_* : \bar{\alpha} \rightarrow \bar{z} \quad (20)$$

$$\bar{\alpha} \mapsto [\tilde{P}_{k_1}^Q(A_1, b_1)(\alpha_1) \mid \tilde{P}_{k_2}^Q(A_2, b_2)(\alpha_2) \mid \dots \mid \tilde{P}_{k_n}^Q(A_n, b_n)(\alpha_n)] = \bar{z} \quad (21)$$

Again, notions of cardinality and dimension can be easily defined:

$$\text{Card}(\mathbb{P}) = \sum_{i=1}^n \text{Card}(\tilde{P}_{k_i}^Q(A_i, b_i)) \quad (22)$$

$$\text{Dim}(\mathbb{P}) = \sum_{i=1}^n \text{Dim}(\tilde{P}_{k_i}^Q(A_i, b_i)) \quad (23)$$

3. Bounds

To ensure that the nodes indeed lie within the domain of the optimization element, it is necessary to introduce bounds for the parameters. Naturally, the bounds on the natural coordinates are easiest to compute. Then, by using the inverse map of P_k^Q bounds on the parameters for each symmetry orbit can be found. Because of the potentially complex structure of the natural coordinates, bounds for the parameters of the k th symmetry orbit are given as a set of two matrix-vector inequalities:

$$B_{u,k} \xi \leq d_{u,k} \quad (24)$$

$$B_{l,k} \xi \geq d_{l,k} \quad (25)$$

These bounds can be easily converted to the constrained case as well by simply using the definition of $\tilde{P}_k^Q(A, b)$ in eq. (14). Namely,

$$\tilde{B}_{u,k} = B_{u,k} A \quad (26)$$

$$\tilde{d}_{u,k} = d_{u,k} - (B_{u,k} b) \quad (27)$$

$$\tilde{B}_{l,k} = B_{l,k} A \quad (28)$$

$$\tilde{d}_{l,k} = d_{l,k} - (B_{l,k} b) \quad (29)$$

where the variables with tildes represent the constrained matrices and vectors. Bounds on symmetry orbit collections may very easily be created by simply stacking the vectors d_u and d_l and creating a block diagonal

matrix of the matrices B_u and B_l . In particular,

$$\mathbb{B}_u = \begin{bmatrix} B_{u,k_1} & & & \\ & B_{u,k_2} & & \\ & & \ddots & \\ & & & B_{u,k_n} \end{bmatrix} \quad \mathbb{B}_l = \begin{bmatrix} B_{l,k_1} & & & \\ & B_{l,k_2} & & \\ & & \ddots & \\ & & & B_{l,k_n} \end{bmatrix} \quad (30)$$

$$d_u = \begin{bmatrix} d_{u,k_1} \\ d_{u,k_2} \\ \vdots \\ d_{u,k_n} \end{bmatrix} \quad d_l = \begin{bmatrix} d_{l,k_1} \\ d_{l,k_2} \\ \vdots \\ d_{l,k_n} \end{bmatrix} \quad (31)$$

Then, once the symmetry orbit collection, \mathbb{P} , is chosen, the bounds on the parameter vector $\bar{\alpha}$ will be given by:

$$\mathbb{B}_u \bar{\alpha} \leq d_u \quad (32)$$

$$\mathbb{B}_l \bar{\alpha} \geq d_l \quad (33)$$

4. An Example

To illustrate the above framework, the triangle will be used as a working example. From here onwards, Δ will be used to denote the triangle. First, the mapping R from the natural coordinates to the physical coordinates can be defined as in eq. (2). In the case of the triangle, the natural coordinates are the standard barycentric coordinates which indicate the distance between the point and each of the three vertices. So, for this coordinate system, the mapping R is defined by N and ν which are given as,

$$N = \begin{bmatrix} -1 & 1 & -1 \\ -1 & -1 & 1 \end{bmatrix}, \quad \nu = \begin{bmatrix} 0 \\ 0 \end{bmatrix} \quad (34)$$

then, each P_k^Δ can be defined for each symmetry orbit by defining all $S_{k,i}$ and $\sigma_{k,i}$:

$$S_{1,1} = \emptyset, \quad \sigma_{1,1} = \begin{bmatrix} \frac{1}{3} \\ \frac{1}{3} \\ \frac{1}{3} \end{bmatrix} \quad (35)$$

$$S_{2,1} = \begin{bmatrix} 1 \\ 1 \\ -2 \end{bmatrix}, \quad \sigma_{2,1} = \begin{bmatrix} 0 \\ 0 \\ 1 \end{bmatrix}; \quad S_{2,2} = \begin{bmatrix} 1 \\ -2 \\ 1 \end{bmatrix}, \quad \sigma_{2,2} = \begin{bmatrix} 0 \\ 1 \\ 0 \end{bmatrix}; \quad S_{2,3} = \begin{bmatrix} -2 \\ 1 \\ 1 \end{bmatrix}, \quad \sigma_{2,3} = \begin{bmatrix} 1 \\ 0 \\ 0 \end{bmatrix} \quad (36)$$

$$S_{3,1} = \begin{bmatrix} 1 & 0 \\ 0 & 1 \\ -1 & -1 \end{bmatrix}, \quad \sigma_{3,1} = \begin{bmatrix} 0 \\ 0 \\ 1 \end{bmatrix}; \quad S_{3,2} = \begin{bmatrix} 0 & 1 \\ 1 & 0 \\ -1 & -1 \end{bmatrix}, \quad \sigma_{3,2} = \begin{bmatrix} 0 \\ 0 \\ 1 \end{bmatrix}; \quad S_{3,3} = \begin{bmatrix} -1 & -1 \\ 1 & 0 \\ 0 & 1 \end{bmatrix}, \quad \sigma_{3,3} = \begin{bmatrix} 1 \\ 0 \\ 0 \end{bmatrix} \quad (37)$$

$$S_{3,4} = \begin{bmatrix} 1 & 0 \\ -1 & -1 \\ 0 & 1 \end{bmatrix}, \quad \sigma_{3,4} = \begin{bmatrix} 0 \\ 1 \\ 0 \end{bmatrix}; \quad S_{3,5} = \begin{bmatrix} 0 & 1 \\ -1 & -1 \\ 1 & 0 \end{bmatrix}, \quad \sigma_{3,5} = \begin{bmatrix} 0 \\ 1 \\ 0 \end{bmatrix}; \quad S_{3,6} = \begin{bmatrix} -1 & -1 \\ 0 & 1 \\ 1 & 0 \end{bmatrix}, \quad \sigma_{3,6} = \begin{bmatrix} 1 \\ 0 \\ 0 \end{bmatrix} \quad (38)$$

From the definitions of $S_{k,i}$ and $\sigma_{k,i}$ it can be seen that:

$$\text{Card}(P_1^\Delta) = 1, \quad \text{Dim}(P_1^\Delta) = 0 \quad (39)$$

$$\text{Card}(P_2^\Delta) = 3, \quad \text{Dim}(P_2^\Delta) = 1 \quad (40)$$

$$\text{Card}(P_3^\Delta) = 6, \quad \text{Dim}(P_3^\Delta) = 2 \quad (41)$$

To get a sense for the structure of the symmetry orbits, a few plots are given below:

It should be noted that in these plots, the mapping shown is a composition of R and P_k^Δ to create nodes in the physical domain from the parameters. To ensure that the points do indeed lie within the

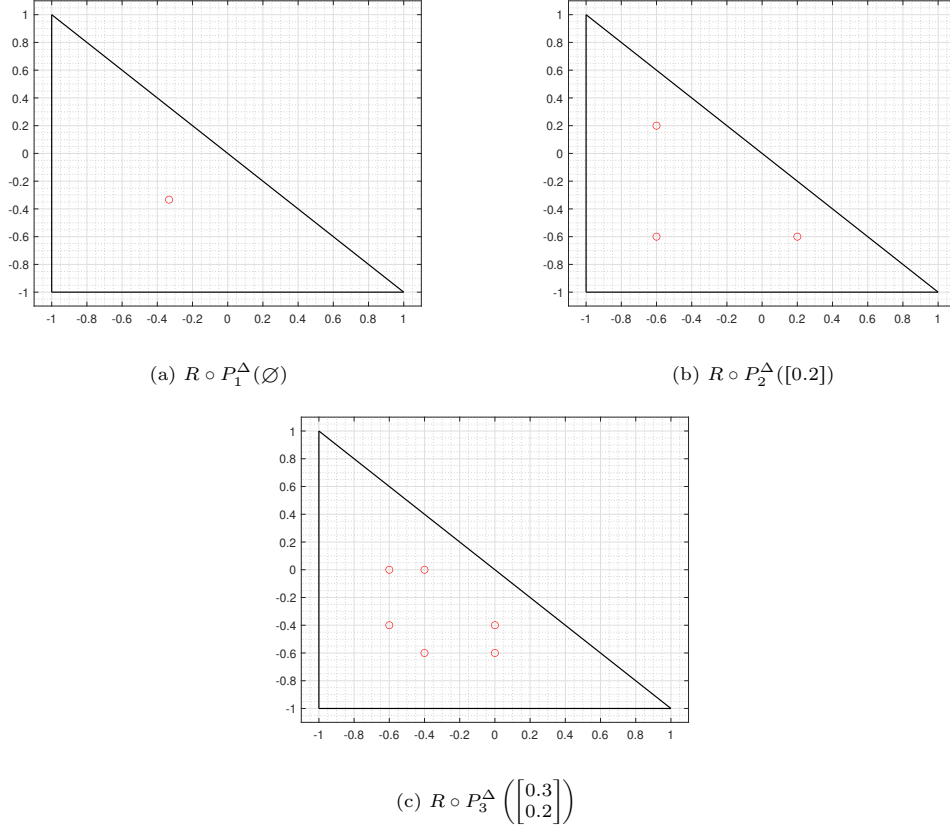


Figure 1: Some symmetry orbits within the triangle

triangle constraints are given on the barycentric coordinates. Denoting the three barycentric coordinates by λ_1, λ_2 , and λ_3 , the constraints on these coordinates are given by:

$$0 \leq \lambda_i \leq 1, \quad \lambda_1 + \lambda_2 + \lambda_3 = 1 \quad (42)$$

From the definition of the symmetry orbits, the second criterion is automatically fulfilled. However, translating the first inequality into bounds on the parameters is slightly more complex and results in the following constraints for each symmetry orbit:

$$B_{u,1} = \emptyset = B_{1,1}, \quad d_{u,1} = \emptyset = d_{1,1}; \quad (43)$$

$$B_{u,2} = [1] = B_{1,2}, \quad d_{u,2} = \left[\frac{1}{2}\right], \quad d_{1,2} = [0]; \quad (44)$$

$$B_{u,3} = \begin{bmatrix} 1 & 0 \\ 0 & 1 \\ -1 & -1 \end{bmatrix} = B_{1,3}, \quad d_{u,3} = \begin{bmatrix} 1 \\ 1 \\ 0 \end{bmatrix}, \quad d_{1,3} = \begin{bmatrix} 0 \\ 0 \\ -1 \end{bmatrix} \quad (45)$$

Now, for a comprehensive example consider a polyhedra symmetry orbit collection composed of both constrained and free symmetry orbits. In this example, consider constraining some of the nodes to lie on the boundary. In particular, working off of the third symmetry orbit, one of the ways this could occur is when the parameters ξ are of the form:

$$\xi = \begin{bmatrix} \alpha \\ 0 \end{bmatrix} \quad (46)$$

for some a . Now creating a constrained symmetry orbit satisfying this is simpler. Namely,

$$A = \begin{bmatrix} 1 \\ 0 \end{bmatrix} \quad b = \begin{bmatrix} 0 \\ 0 \end{bmatrix} \quad (47)$$

$$\tilde{P}(A, b)(\alpha) = \begin{bmatrix} 1 \\ 0 \end{bmatrix} [\alpha] + \begin{bmatrix} 0 \\ 0 \end{bmatrix} = \begin{bmatrix} \alpha \\ 0 \end{bmatrix} \quad (48)$$

From this computation and eqs. (16) and (17) it is clear that:

$$\text{Card}(\tilde{P}_3^\Delta(A, b)) = 6, \quad \text{Dim}(\tilde{P}_3^\Delta(A, b)) = 1 \quad (49)$$

and from eqs. (26)-(29), it can be seen that:

$$B_{u,3} = \begin{bmatrix} 1 \\ 0 \\ -1 \end{bmatrix} = B_{l,3}, \quad d_{u,3} = \begin{bmatrix} 1 \\ 1 \\ 0 \end{bmatrix}, \quad d_{l,3} = \begin{bmatrix} 0 \\ 0 \\ -1 \end{bmatrix} \quad (50)$$

Now to proceed with the example, let \mathbb{P} be a symmetry orbit collection $\bar{\alpha}$ a set of constrained parameters defined as:

$$\mathbb{P} = (P_1^\Delta(Id, \mathbf{0}), P_2^\Delta(Id, \mathbf{0}), P_2^\Delta(Id, \mathbf{0}), P_3^\Delta(Id, \mathbf{0}), P_3^\Delta(A, b)) \quad (51)$$

$$\bar{\alpha} = \begin{bmatrix} 0.25 \\ 0.5 \\ 0.1 \\ 0.6 \\ 0.7 \end{bmatrix} \quad (52)$$

Where A and b are defined as above. Then, the to ensure this collection of alphas lies within the element, the following inequalities can be checked:

$$\begin{bmatrix} 0 \\ 0 \\ 0 \\ 0 \\ -1 \\ 0 \\ 0 \\ -1 \end{bmatrix} \leq \begin{bmatrix} 1 & & & & & & & \\ & 1 & & & & & & \\ & & 1 & 0 & & & & \\ & & 0 & 1 & & & & \\ & & -1 & -1 & & & & \\ & & & & 1 & & & \\ & & & & 0 & & & \\ & & & & -1 & & & \end{bmatrix} \bar{\alpha} \leq \begin{bmatrix} \frac{1}{2} \\ \frac{1}{2} \\ \frac{1}{2} \\ 1 \\ 1 \\ 0 \\ 1 \\ 0 \end{bmatrix} \quad (53)$$

These indeed hold, resulting in the following z values for $\mathbb{P}_*(\bar{\alpha})$:

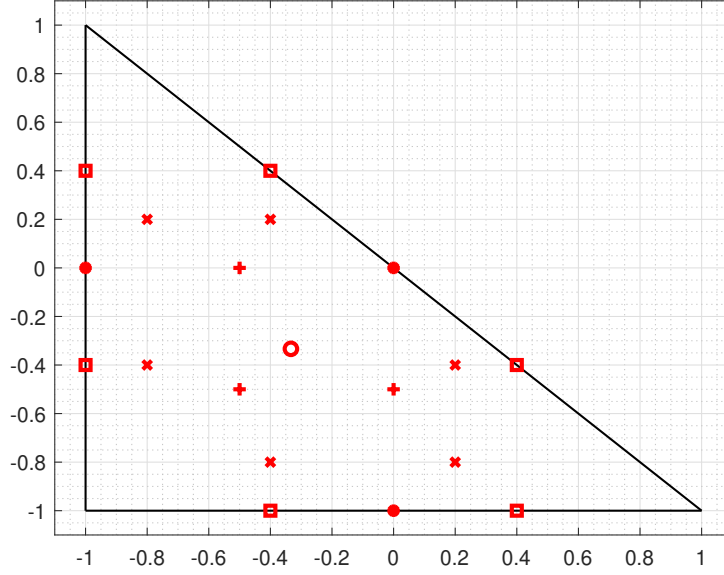


Figure 2: Nodes created by \mathbb{P}_* $\left(\begin{bmatrix} 0.25 \\ 0.5 \\ 0.1 \\ 0.6 \\ 0.7 \end{bmatrix} \right)$

5. Optimization

From the notions described above, the optimization problem can now be defined. For a given Symmetry Orbit Collection, \mathbb{P} , and an objective function, f , the optimization problem is given by:

$$\min_{\bar{\alpha}} f(\mathbb{P}_*(\bar{\alpha})) \quad (54a)$$

$$\text{s.t. } \mathbb{B}_u \bar{\alpha} \leq d_u, \quad (54b)$$

$$\mathbb{B}_l \bar{\alpha} \geq d_l \quad (54c)$$

5.1. Objective Function

In this paper, the main objective function that was used was the Lebesgue constant. Given a nodal distribution in an element Q ,

$$z = (z_1, z_2, \dots, z_n) \quad (55)$$

define the usual Lagrange basis polynomials $\ell_i(x)$ for each z_i . Then, the Lebesgue constant is defined as,

$$\Lambda(z) = \max_{x \in Q} \sum_{i=1}^n |\ell_i(x)| \quad (56)$$

5.2. Fixing Nodes from Lower Dimensions

As mentioned before, it is often desirable to fix some nodes on the boundaries, faces, and vertices of an element. Specifically, it is helpful to require these nodes to obey an already existing lower-dimensional distribution. The process of achieving this is, however, deceptively complex. It will be helpful to denote the element by Q .

Here, a brute force algorithm is used. First, the nodes must be projected from the lower to the higher dimensional element. So, a face type of Q is chosen. Then, a nodal distribution from the element type of the face is projected onto each face of this type in Q . This distribution will be denoted by $z = (z_1, z_2, \dots, z_n)$.

Next, pick a z_i . The next goal is to find a vector of parameters ξ and the correct symmetry orbit such that z_i can be recovered from ξ . To do this, it is first necessary to find the best approximation for each symmetry orbit. Because of their complex matrix structure, linear least squares problem for the **first** point in each unconstrained symmetry orbit of Q is solved,

$$\xi_k = \arg \min_{\xi} \|NS_1^k \xi + N\sigma_1^k + \nu - z_i\| \quad (57)$$

where S_1^k and σ_1^k are as defined in eq. (4) and N and ν are as defined in eq. (2). Only solving for the first point in each symmetry orbit ensures no double counting of symmetry orbits. Solving these least squares problems results in a collection, $\Xi = \{\xi_k\}$ of parameter vectors. To ensure that the solutions to the least squares problems can indeed recover z_i and create physical nodes that lie with the element, let

$$\mathcal{I}_i = \{k : \|NS_1^k \xi_k + N\sigma_1^k + \nu - z_i\| < \epsilon, B_u \xi_k \leq d_u, B_l \xi_k \geq d_l\} \quad (58)$$

for some small $\epsilon > 0$. It should be noted that this collection could be (and very often is) empty. If this is the case, remove z_i from z and choose a different z_j .

Now, if \mathcal{I}_i is non-empty for z_i , it is desired to choose the smallest possible symmetry orbit containing to avoid redundancies. Thus, let

$$\kappa_i = \min \mathcal{I}_i, \quad \alpha_i = \xi_{\kappa_i} \quad (59)$$

and remove z_i from z . This process is repeated until z is empty.

This procedure results in two sets, $\{\alpha_i\}$ and $\{\kappa_i\}$. Relabelling i 's such that α_i still corresponds to κ_i , but i takes on all positive integer values up to some non-zero value (say n), yields the desired sets. From these two sets, a polyhedra symmetry orbit collection, \mathbb{P} consisting of exactly the constrained polyhedra symmetry orbits necessary to create the lower-dimensional distribution on **each** face type of Q can be constructed:

$$\mathbb{P} = (\tilde{P}_{\kappa_1}^Q(\mathbf{0}, \alpha_1), \tilde{P}_{\kappa_2}^Q(\mathbf{0}, \alpha_2), \dots, \tilde{P}_{\kappa_n}^Q(\mathbf{0}, \alpha_n)) \quad (60)$$

5.3. Possible Symmetry Orbit Collections

Once given a Symmetry Orbit Collection, it is now clear how to solve the optimization problem. However, how those collections come about should be discussed. Once the desired polynomial degree and the type of element is known, the number of total desired nodes, n can be easily calculated. Given this, for an element with m different symmetry orbits, all integer vector solutions c to the equation:

$$[\text{Card}(P_1^Q), \text{Card}(P_2^Q), \dots, \text{Card}(P_m^Q)] \cdot c = n \quad (61)$$

will give all possible unconstrained symmetry orbit collections, which could then be optimized over. Given a collection of constrained symmetry orbits, $\mathbb{P}_{\text{constr}}$, that are already prescribed (from fixing nodes from lower dimensions, requiring nodes to be on faces, or other constraints), with a total of n desired nodes, all integer vector solutions c to the equation:

$$[\text{Card}(P_1^Q), \text{Card}(P_2^Q), \dots, \text{Card}(P_m^Q)] \cdot c = n - \text{Card}(\mathbb{P}_{\text{constr}}) \quad (62)$$

will yield all possible unconstrained symmetry orbits, \mathbb{P}_{free} , such that,

$$\mathbb{P} = \mathbb{P}_{\text{free}} \cup \mathbb{P}_{\text{constr}} \quad (63)$$

will grant the desired number of nodes and can easily be optimized over.

6. Numerical experiments

Several numerical experiments were performed. In particular, optimization was performed on a variety of different element types. These include the line in one dimension, the triangle and the quadrilateral in two dimensions, and the tetrahedron, hexahedron, and triangular prism in three dimensions. For each different element, the optimized nodal distributions Lebesgue constant was compared to that of the standard uniform distribution. When applicable (namely when working with tensor product type elements), the optimized distribution was also compared to the tensored Gauss-Legendre-Lobatto (GLL) distribution. The results are shown below. It should also be noted that for two and three dimensional elements, the nodes on the edges (resp. faces) were fixed to obey the optimized nodal distributions generated for their respective lower dimensional element to easily allow conformity between elements within a mesh.

6.1. 1D Experiments

In one dimension, the optimization yielded distributions with much lower Lebesgue constants than the uniform distribution, as shown in Fig. 3. Furthermore, when directly comparing the Lebesgue constants of the optimized distributions and the standard GLL nodal distributions, shown in Fig. 4, it can be seen that the Lebesgue constants of the optimized distributions is lower than that of the GLL distributions.

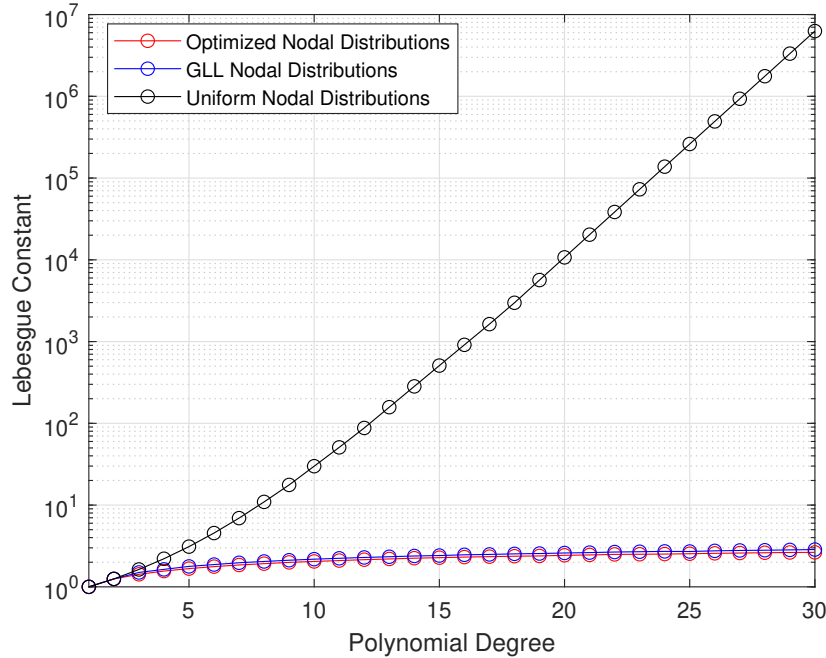


Figure 3: Optimized nodal distributions compared with GLL and uniform nodal distributions via the Lebesgue constant for the line.

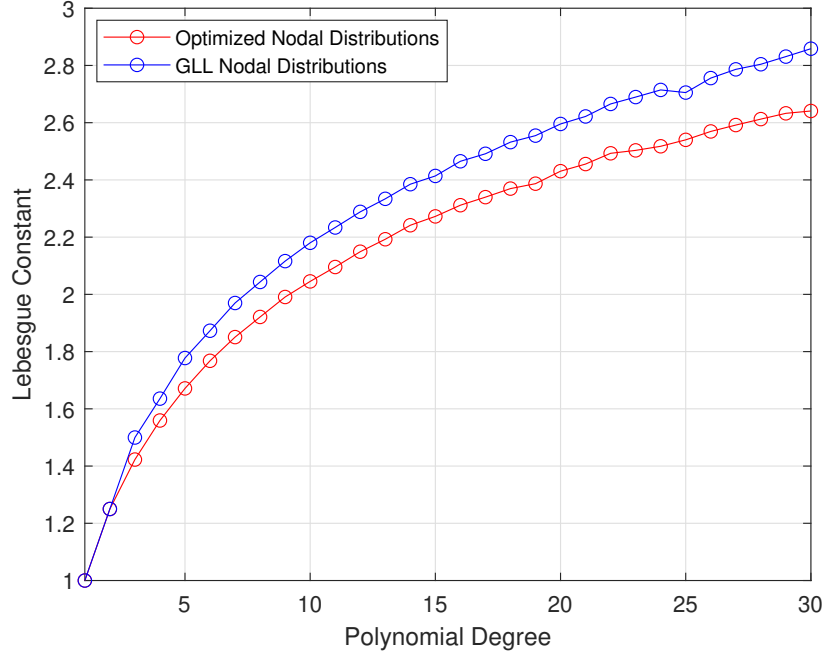


Figure 4: Direct comparison of optimized and GLL nodal distributions for the line.

6.2. 2D Experiments

In two dimensions, optimized distributions were generated for both the triangle and the quadrilateral.

The optimized distributions' Lebesgue constants were compared with those of uniform distributions for the triangle in Fig. 5. For further clarity, the optimized distributions' Lebesgue constants were also plotted without comparison in Fig. 6. Due to there being no other standard distributions for the triangle, this was the only distribution used for comparison. Additionally, for the sake of visualization, the explicit optimized nodal distribution is shown in Fig. 7 for polynomial degree 9.

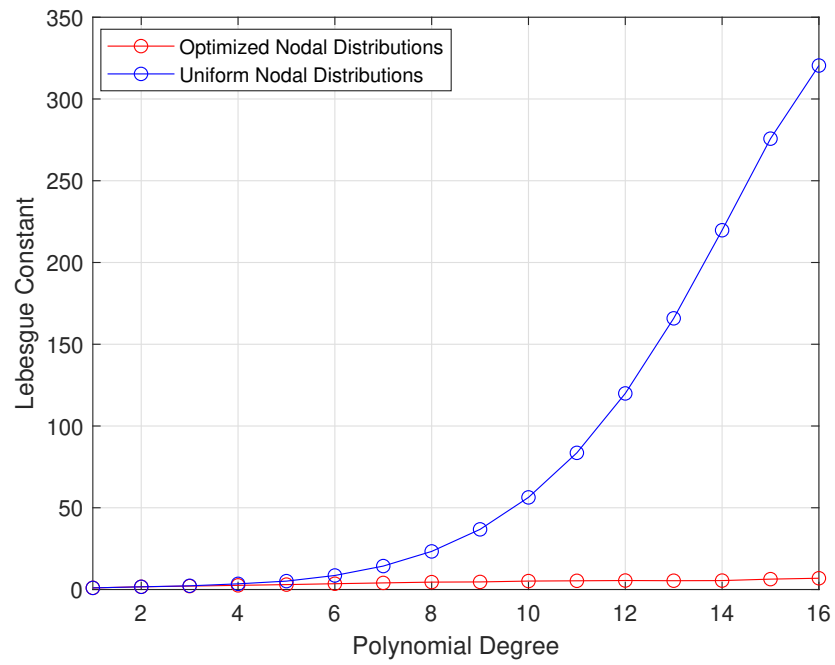


Figure 5: Optimized Lebesgue constant as a function of polynomial degree for both uniform and optimized nodal distributions for the triangle.

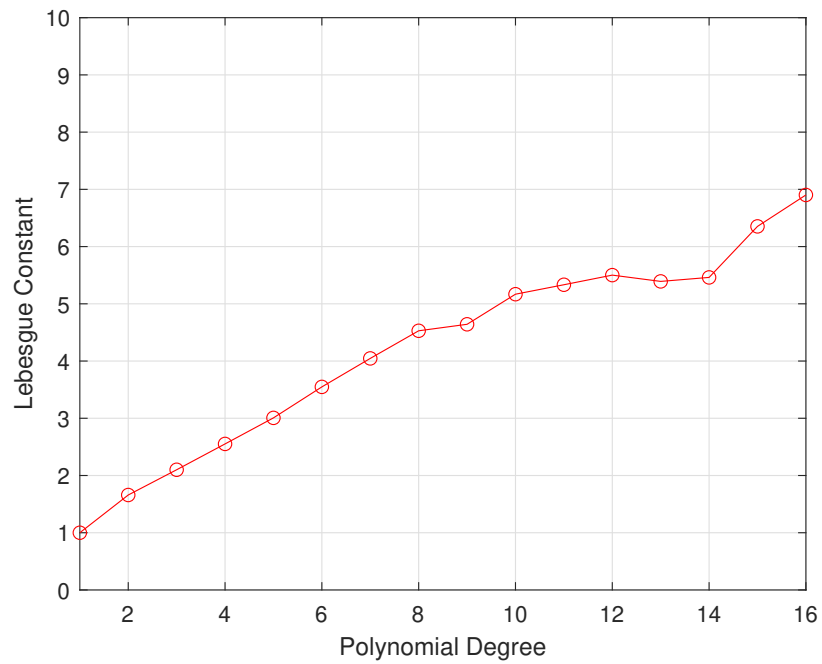


Figure 6: Optimized Lebesgue constant as a function of polynomial degree for the triangle.

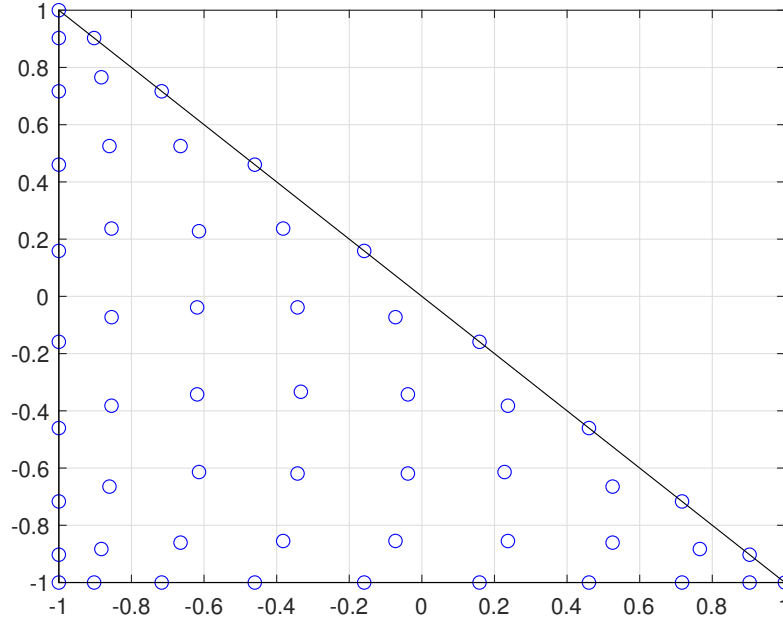


Figure 7: Optimized distribution for the degree 9 triangle.

For the quadrilateral, the optimized distributions' Lebesgue constants were compared with those of uniform distributions and two dimensional GLL distributions in Fig. 8. For clarity, the optimized distributions were also compared to only the GLL distributions in Fig. 9. Again, for visualization, the explicit optimized nodal distribution is shown in Fig. 10 for polynomial degree 9.

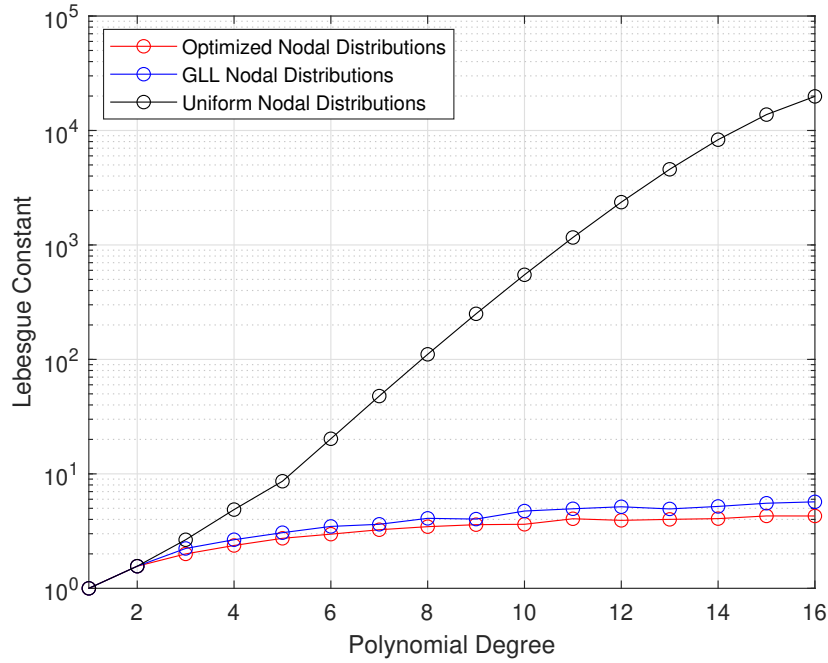


Figure 8: Optimized nodal distributions compared with GLL and uniform nodal distributions via the Lebesgue constant for the quadrilateral.

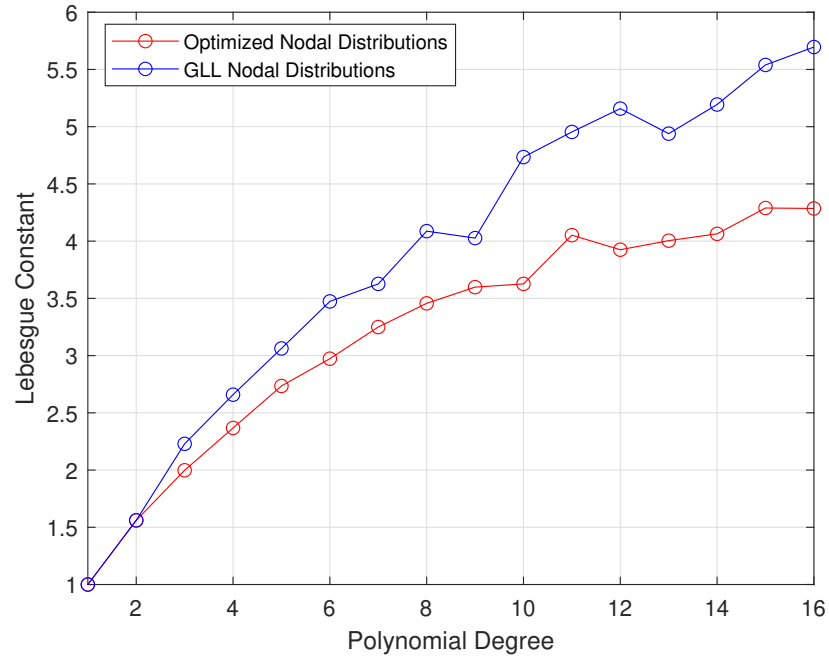


Figure 9: Direct comparison of optimized and GLL nodal distributions for the quadrilateral.

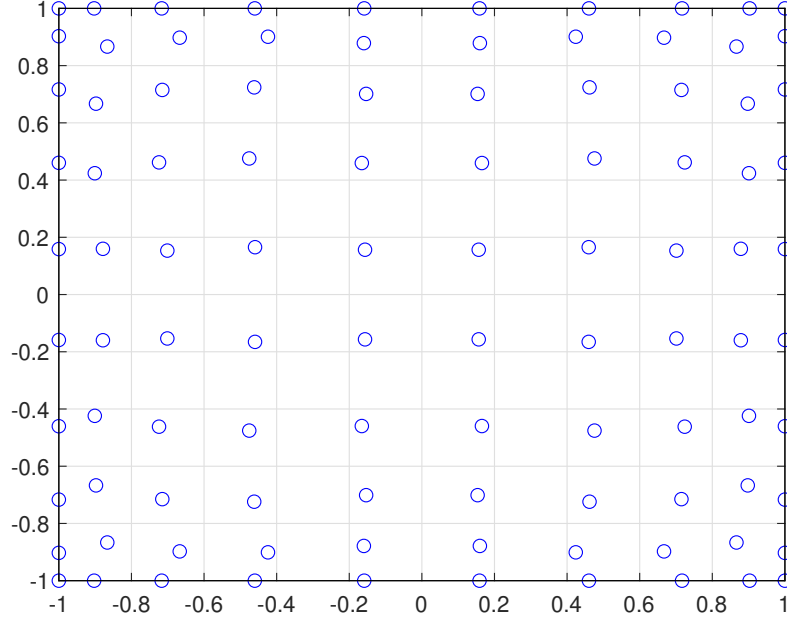


Figure 10: Optimized distribution for the degree 9 quadrilateral.

6.3. 3D Experiments

In three dimensions, optimized distributions were generated for the tetrahedron, the hexahedron, and the triangular prism.

The optimized distributions' Lebesgue constants were compared with those of uniform distributions for the tetrahedron in Fig. 11. Due to there again being no other standard distributions for the triangle, this was the only distribution used for comparison. For the sake of visualization, the explicit optimized nodal distribution is shown in Fig. 12 for polynomial degree 5.

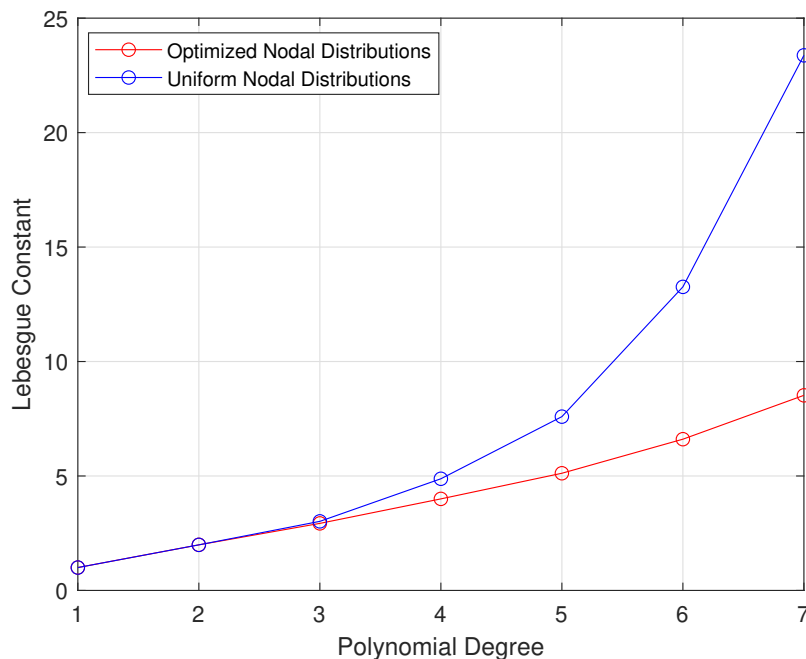


Figure 11: Optimized nodal distributions compared with uniform nodal distributions via the Lebesgue constant for the tetrahedron.

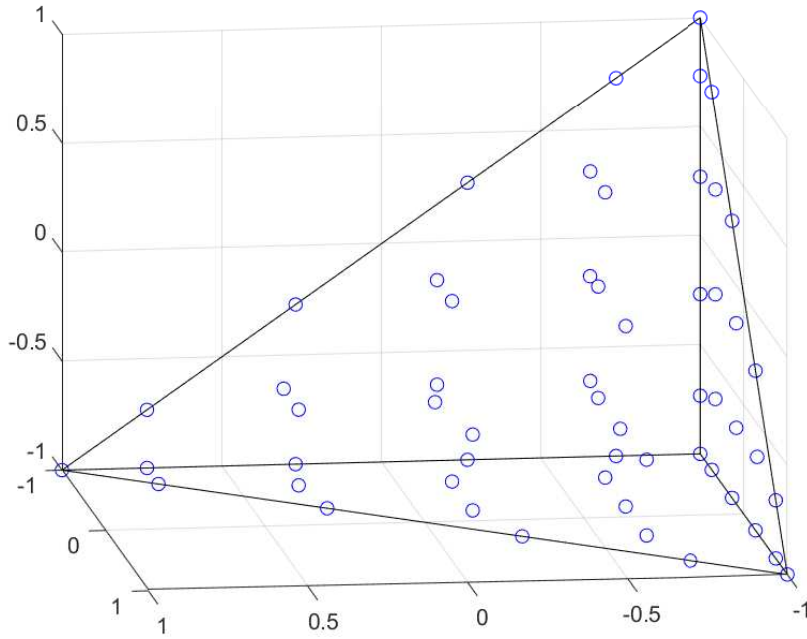


Figure 12: Optimized distribution for the degree 5 tetrahedron.

For the hexahedron, the optimized distributions' Lebesgue constants were compared with those of uniform distributions and three dimensional GLL distributions in Fig. 13. For clarity, the optimized distributions were also directly compared to the GLL distributions in Fig. 14. Again, for visualization, the explicit optimized nodal distribution is shown in Fig. 15 for polynomial degree 5.

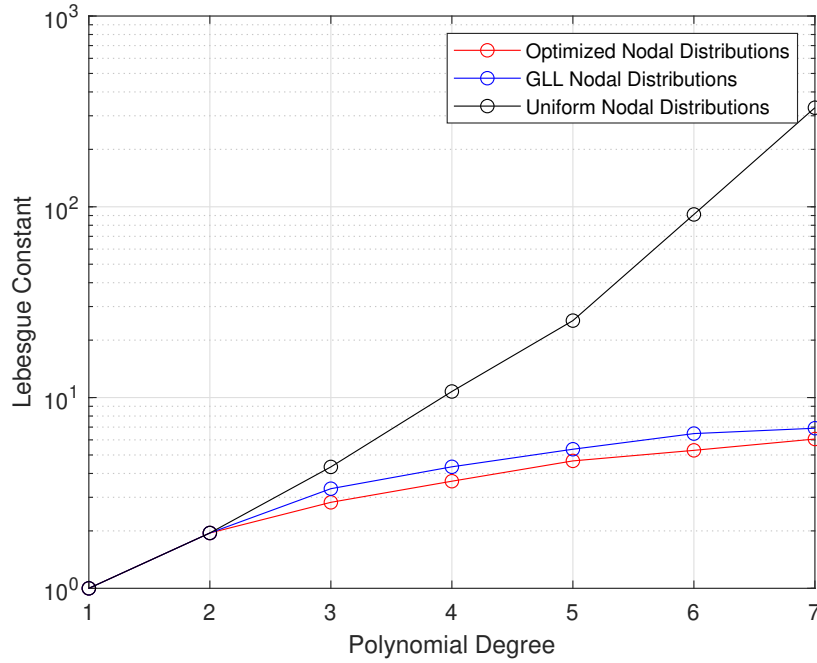


Figure 13: Optimized nodal distributions compared with GLL and uniform nodal distributions via the Lebesgue constant for the hexahedron.

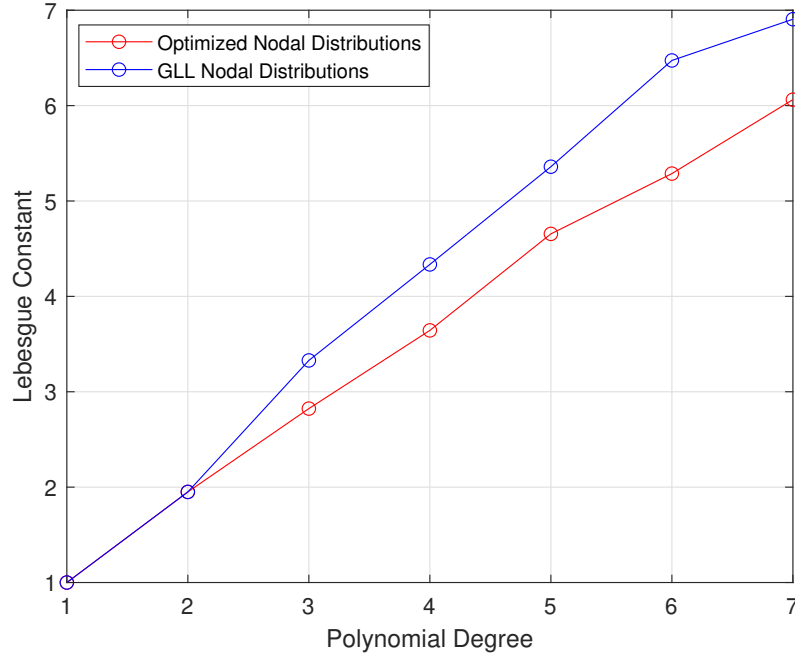


Figure 14: Direct comparison of optimized and GLL nodal distributions for the hexahedron.

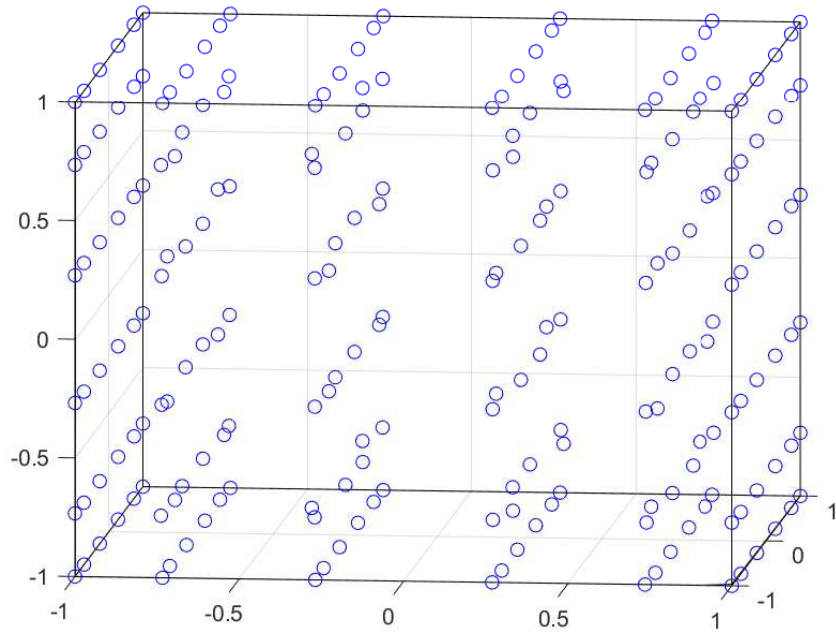


Figure 15: Optimized distribution for the degree 5 hexahedron.

Finally, the optimized distributions' Lebesgue constants were compared with those of uniform distributions for the triangular prism in Fig. 16. Since there again was no other standard distributions, this was the only distribution used for comparison. The explicit optimized nodal distribution is also shown in Fig. 17 for polynomial degree 5.

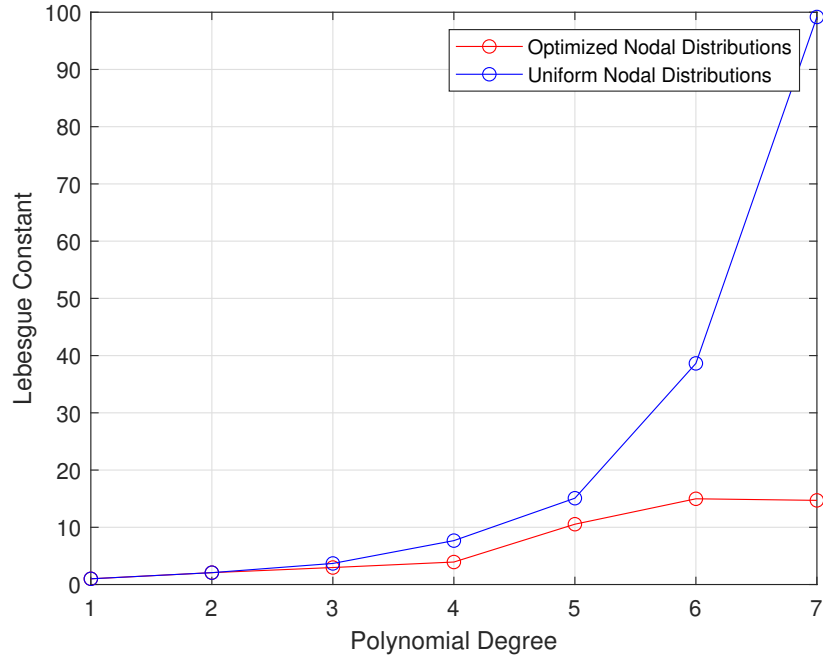


Figure 16: Direct comparison of optimized and uniform nodal distributions for the triangular prism.

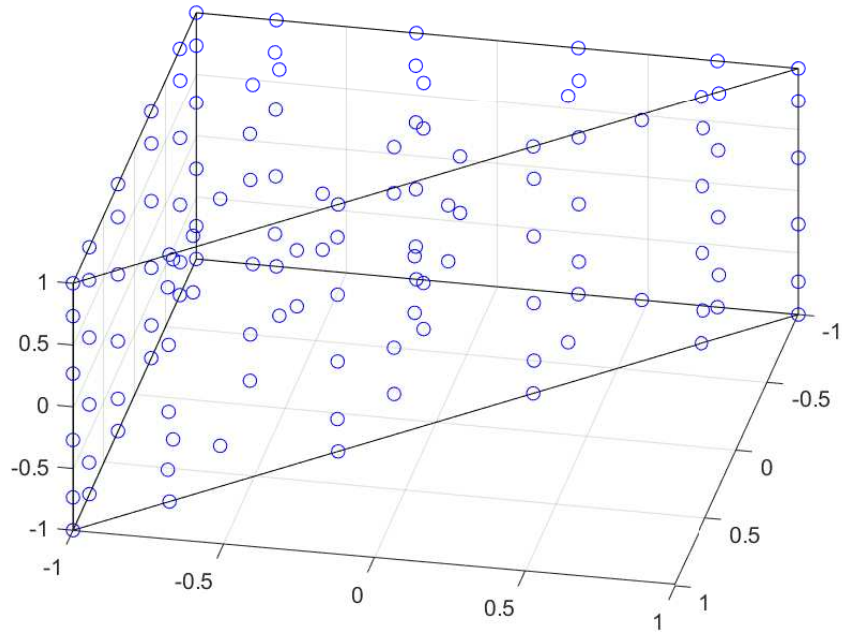


Figure 17: Optimized distribution for the degree 5 triangular prism.

7. Conclusion

In this paper, we introduce a new numerical framework that can be used to optimize nodal distributions for general elements with respect to any desired parameter. In particular, we used the Lebesgue constant as

an optimization tool which results in nodal distributions which generate mass matrices with low condition number. This method also ensures conformity between different elements and element types in general finite element meshes by utilizing constrained symmetry orbits to fix edge and face distributions to those of lower dimensional elements. Leveraging symmetry groups allows the elements to retain the desired properties when used in any orientation in meshes. These combined approaches lead to high polynomial degree, well-conditioned, distributions which are irrespective of orientation, while ensuring conformity to other mesh elements and element types.

Additional research is required to extend this approach to other potential optimization parameters, higher dimensional elements, and potentially higher polynomial degrees.

Acknowledgments

This work is supported by AFOSR award numbers FA9550-20-1-0236, FA9550-22-1-0002, FA9550-22-1-0004, and ONR award number N00014-22-1-2299. The content of this publication does not necessarily reflect the position or policy of any of these supporters, and no official endorsement should be inferred.

References

- [1] L.P. Bos. Bounding the lebesgue function for lagrange interpolation in a simplex. Journal of Approximation Theory, 38(1):43–59, 1983.
- [2] Lp Bos, Mark Taylor, and Beth Wingate. Tensor product gauss-lobatto points are fekte points for the cube. Math. Comput., 70:1543–1547, 10 2001.
- [3] Qi Chen and Ivo Babuška. Approximate optimal points for polynomial interpolation of real functions in an interval and in a triangle. Computer Methods in Applied Mechanics and Engineering, 128(3):405–417, 1995.
- [4] D. A. Dunavant. High degree efficient symmetrical gaussian quadrature rules for the triangle. International Journal for Numerical Methods in Engineering, 21(6):1129–1148, 1985.
- [5] Leopold Fejér. Bestimmung derjenigen abszissen eines intervalles, für welche die quadratsumme der grundfunktionen der lagrangeschen interpolation im intervalle ein möglichst kleines maximum besitzt. Annali della Scuola Normale Superiore di Pisa - Classe di Scienze, 1(3):263–276, 1932.
- [6] M. Fekete. Über die Verteilung der Wurzeln bei gewissen algebraischen Gleichungen mit ganzzahligen Koeffizienten. Math. Z., 17(1):228–249, 1923.
- [7] J. S. Hesthaven. From electrostatics to almost optimal nodal sets for polynomial interpolation in a simplex. SIAM Journal on Numerical Analysis, 35(2):655–676, 1998.
- [8] J. S. Hesthaven and C. H. Teng. Stable spectral methods on tetrahedral elements. SIAM Journal on Scientific Computing, 21(6):2352–2380, 2000.
- [9] Jan Hesthaven. From electrostatics to almost optimal nodal sets for polynomial interpolation in a simplex. SIAM J. Numer. Anal., 35, 02 1997.
- [10] Jan Hesthaven and Tim Warburton. Nodal Discontinuous Galerkin Methods: Algorithms, Analysis, and Applications, volume 54. 01 2007.
- [11] Tobin Isaac. Recursive, parameter-free, explicitly defined interpolation nodes for simplices, 02 2020.
- [12] Jingliang Li, Heping Ma, Yonghui Qin, and Shuaiyin Zhang. A spectral method for triangular prism. Applied Numerical Mathematics, 129:26–38, 2018.
- [13] Youyun Li, Li-Lian Wang, Huiyuan Li, and Heping Ma. A New Spectral Method on Triangles, volume 76, pages 237–246. 10 2010.

- [14] J. Lyness and Ronald Cools. A survey of numerical cubature over triangles. Proceedings of Symposia in Applied Mathematics American Mathematical Society Providence, RI, 48, 04 1994.
- [15] Richard Pasquetti and Francesca Rapetti. Spectral element methods on triangles and quadrilaterals: comparisons and applications. Journal of Computational Physics, 198(1):349–362, 2004.
- [16] M. A. Taylor, B. A. Wingate, and R. E. Vincent. An algorithm for computing fekte points in the triangle. SIAM Journal on Numerical Analysis, 38(5):1707–1720, 2000.
- [17] Mark Taylor and Beth Wingate. Generalized diagonal mass matrix spectral element method for non-quadrilateral elements. Applied Numerical Mathematics - APPL NUMER MATH, 33:259–265, 05 2000.
- [18] S. Wandzurat and H. Xiao. Symmetric quadrature rules on a triangle. Computers & Mathematics with Applications, 45(12):1829–1840, 2003.
- [19] F.D. Witherden and P.E. Vincent. On the identification of symmetric quadrature rules for finite element methods. Computers & Mathematics with Applications, 69(10):1232–1241, 2015.